

BUBBLE CHARACTERISTICS IN AN INTERNALLY CIRCULATING FLUIDIZED BED

YOUNG T. CHOI AND SANG D. KIM

Department of Chemical Engineering, Korea Advanced Institute of Science and Technology, Seoul 130-650, Korea

Key Words: Solids Circulation Rate, Bubble Properties, Circulating Fluidized Bed

In an internally circulating fluidized bed, the bubble properties (bubble chord length, volume fraction, rising velocity and frequency) in the fluidized bed and the solids circulation rate from a fluidized bed to a moving bed were determined, along with the effects of gas velocity on solids circulation rate and bubble properties in the fluidized bed. The solids circulation rate increases with increase in gas velocity. The measured bubble chord length distribution in the fluidized bed is well represented by the logarithmic normal distribution. The measured bubble chord length, volume fraction and rising velocity increase with bed height and gas velocity to the fluidized bed. However, bubble chord length, volume fraction and local bubble frequency decrease with increasing gas velocity to the moving bed. The bubble chord length, volume fraction and rising velocity are lower in the bed wall region and exhibit a peak value at a dimensionless lateral distance of 0.5–0.8, and the peak moves to the center region of the bed with increasing bed height. The rate of increase in bubble rising velocity increases with bubble size up to about 0.07 m, at which the flow regime may lie between bubbly and slugging flows. The bubble properties in the internally circulating fluidized bed have been correlated with the solids circulation on the basis of theoretical equations in the literature.

Introduction

Recently, circulating fluidized beds have been employed widely in the field of petroleum refining,⁸⁾ coal combustion and gasification, in a fluidized-bed operation in which NO_x and SO₂ formations can be reduced at lower operating temperatures with additives. However, conventional circulating fluidized beds require a very tall main vessel as a solids riser and an accompanying tall cyclone. To reduce the height of the conventional circulating fluidized bed and its construction cost, several new types of circulating fluidized bed using a central draft tube^{11,18)} or flat plates^{9,10)} to divide the bed for internal solids circulation in a single vessel have been developed. In the internally circulating fluidized bed with a partition plate, the solids circulation rate can be easily controlled in a simpler circulation loop at even lower gas velocities. For a combustor, it is required to operate the combustor with a wide range of load which can be controlled by the solids circulation rate. Also, the bubble properties are important parameters in governing the overall performance of a fluidized bed combustor. Therefore, information on the solids circulation rate and bubble properties in the internally circulating fluidized beds are required to predict an optimum operating condition. Bubble properties have been measured by various detecting

devices such as the electroresistivity probe,^{2,4,13)} capacitance probe,^{20–23)} pressure differential probe,³⁾ hot-wire probe,¹⁷⁾ optical probe,¹⁹⁾ and X-ray photography^{14,15)} in gas-solid fluidized bed. However, information on bubble properties in an internally circulating fluidized bed have not been reported to date.

In the present study, the effects of gas velocity on the bubble properties in the fluidized bed and solids circulation rate from a fluidized bed to a moving bed were determined.

1. Experimental

Experiments were carried out in a 0.4 m × 0.2 m cross section and 0.9 m-high Plexiglas sheet of the main bed, and the freeboard was expanded to 0.4 m × 0.8 m × 0.4 m high with a conical transition section (0.2 m height) for reducing particle entrainment, as shown schematically in Fig. 1. The apparatus consisted of four sections: air plenum, distributor, main bed and expanded freeboard sections. The main bed was divided into two size-equivalent beds (0.2 m × 0.2 m) by inserting a flat partition plate (0.2 m × 0.45 m) above the distributor so that one section became a fluidized bed in which solid particles moved upward and the other section became a moving bed in which solid particles moved downward at less than the minimum fluidizing velocity. The distance between the distributor and the top of the partition plate was 0.65 m. With this arrangement, an orifice

* Received July 7, 1990. Correspondence concerning this article should be addressed to S. D. Kim.

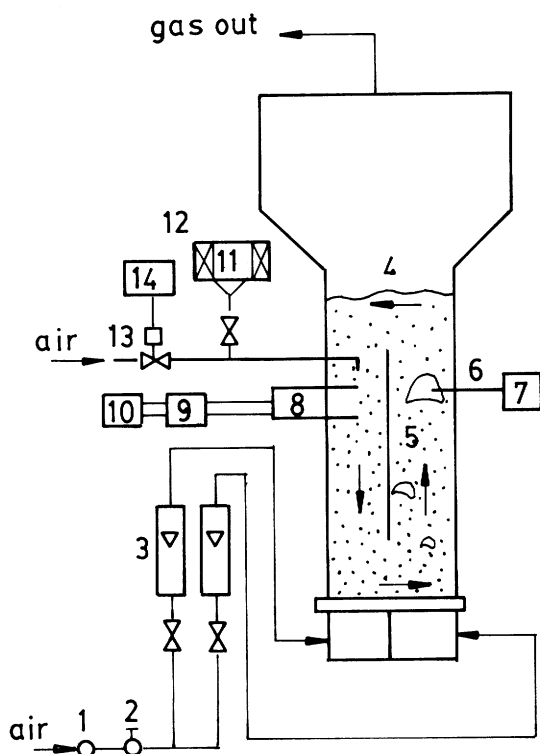


Fig. 1. Schematic diagram of experimental apparatus
 1. oil filter 8. thermistor probe
 2. pressure regulator 9. bridge circuit
 3. flow meter 10. X-Y recorder
 4. main bed 11. hopper
 5. partition plate 12. electrical heater
 6. optical fiber probe 13. solenoid valve
 7. bubble measuring system 14. pulse current generator

opening area (0.04 m^2) between the distributor and the bottom of the partition plate could be made for solids recirculation. Solid particles were supported on a bubble cap distributor which contained 9 bubble caps in which there were $4 \times 2.5 \text{ mm}$ -diameter holes around each bubble cap in the fluidized bed section. In the moving bed section was a perforated plate containing 36 evenly spaced holes, 2 mm in diameter, on which a 200-mesh screen sheet was attached to prevent solids weeping. The air plenum was divided into two size-equivalent sections ($0.2 \text{ m} \times 0.2 \text{ m}$) to supply air into the fluidized and moving beds.

Initially, a known weight of sand particles was loaded into the bed and then the particles were fluidized by compressed air which was introduced into the plenum chambers of each bed through a pressure regulator, a filter and flow meters. The physical properties of the sand particles and the experimental variables are listed in **Tables 1** and **2** respectively.

1.1 Measurement of solids circulation rate

The solids circulation rate was determined by measuring the particle downward velocity in the moving bed. Heated bed materials were used as a tracer for measuring the particle downward velocity

Table 1. Physical properties of sand particles

Particle size distribution	0.25–0.42 mm
Mean particle diameter	0.3 mm
Particle density	2600 kg/m^3
Minimum fluidizing gas velocity	0.127 m/s
Bed voidage at minimum fluidizing condition	0.487

Table 2. Experimental variables

Gas velocity	fluidized bed	up to $4.5 U_{mf}$ (0.57 m/s)
	moving bed	up to U_{mf} (0.127 m/s)
Static bed height	0.6 m	
Orifice opening area	0.04 m^2	

in the moving bed by means of two thermistor probes. Two probes were installed at the center of the moving bed at 0.45 m and 0.5 m above the distributor plate. A known volume of heated tracer particles ($1 \times 10^{-5} \text{ m}^3$, 250°C) was injected pneumatically from a hopper into the middle of the moving bed through a centrally located L-shape injection tube at 0.55 m above the distributor plate. Air was supplied to a tube connected to a solenoid valve which was operated by a pulse current generator. When hot sand particles contacted the probe, a change in resistance of the probe was converted into voltage through a bridge circuit and then amplified and recorded with an X-Y recorder. By measuring the time lag (τ) between the peak-to-peak distance of two signals (**Fig. 3c**), the particle downward velocity can be estimated from the known distance between the two probes ($L = 0.05 \text{ m}$) divided by the time lag ($V_m = L/\tau$). In each operating condition, twenty measurement runs were performed to determine the average particle velocity. It was assumed that the velocity measured at the center of the bed represented the average bulk velocity in the moving bed.

The solids circulation rate can be calculated from the relation

$$W_s = \rho_s(1 - \varepsilon_m)V_m A_m \quad (1)$$

where ρ_s , ε_m , V_m , and A_m are respectively the solids density, bed voidage, particle downward velocity and cross-sectional area of the moving bed. Also, ε_m was assumed to be the bed voidage at minimum fluidizing condition (ε_{mf}).

1.2 Measurement of bubble properties

The bubble chord length, bubble volume fraction, local bubble frequency and bubble rising velocity were measured by means of an optical-fiber probe at four axial bed heights (0.1, 0.21, 0.31 and 0.46 m) above the distributor and at five lateral positions (0.1, 0.125, 0.15, 0.175 and 0.188 m) from the partition plate in

the fluidized bed. A schematic diagram of the system for measuring the bubble properties is shown in Fig. 2. The optical fiber probe consisted of two pairs of optical fibers with a diameter of 500 μm . One pair was a light projector from the light source of an He-Ne laser (Japan Laser Co., JLH-RT20U) and the other, at the opposite side, was a light receiver which was connected to two photo transistors (OPTO Electronics Co., ST-1KLB). The clearance between the lower and upper tips of the probe was 4 mm and the distance between the light projector and receiver was 4 mm. These optical fibers were supported by hypodermic needles of 0.6-mm hole diameter and fixed with an epoxy resin in a stainless steel tube of 8 mm ID \times 0.25 m length. The light received was converted into an electric signal by a photo transistor. The output signal was amplified, monitored by an oscilloscope, and delivered via a comparator to a personal computer (IBM/XT) for analysis. The sampling interval of the signals was 500 μs and 180,000 samples were collected during the sampling period of 90 s for each experimental condition.

Typical response signals are shown in Fig. 3. The fluctuating response signals (Fig. 3A) due to the movement of solid particles across the probe were converted into smoothed signals (Fig. 3B) using the comparator. The output voltage was adjusted to 0.0 V in the atmosphere and 5.0 V in a quiescent bed of solid particles with a variable resistor in the comparator circuit.

The individual bubble rising velocity (U_{bi}) was determined from the following relation (Fig. 3):

$$U_{bi} = \Delta S / t_{1i} \quad (2)$$

where ΔS and t_{1i} are the distance and the time lag between the lower and upper tips of the probe respectively.

Individual bubble chord length (l_{vi}) was determined from the following equation:

$$l_{vi} = t_{2i} U_{bi} \quad (3)$$

where t_{2i} is the time duration of a bubble pulse.

The bubble volume fraction (ε_b) was determined from the relation

$$\varepsilon_b = \frac{1}{T} \sum_{i=1}^{N_b} t_{2i} \quad (4)$$

where T is the total measuring time and N_b is the number of bubbles in time T .

The local bubble frequency (f_b) was determined from the number of signals detected per unit time at the probe tips¹³.

2. Results and Discussion

2.1 Solids circulation rate

The effect of gas velocity (U_f) on solids circulation

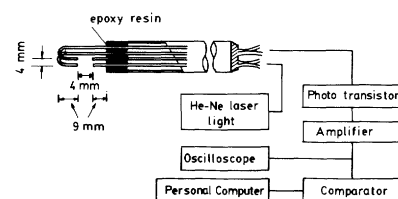


Fig. 2. Schematic diagram of optical-fiber probe system

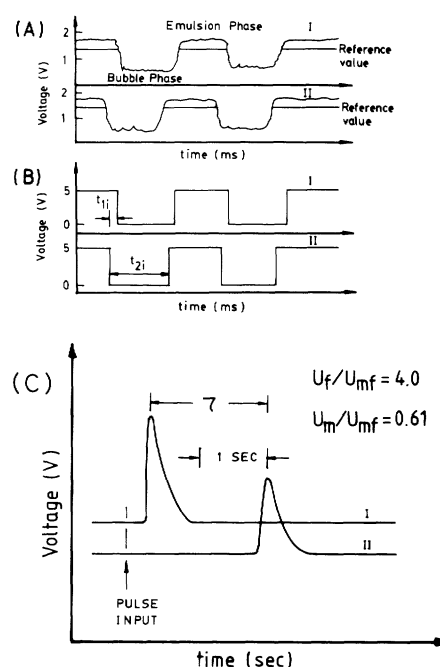


Fig. 3. Typical response signals from optical-fiber and thermistor probes

(A) raw signal (B) smoothed signal by comparator

I: upper tip, II: lower tip

(C) response signal from the thermistor probe

I: upper probe, II: lower probe

rate (W_s) in the bed is shown in Fig. 4A. As can be seen, W_s increases with increasing U_f due to the increase of bed density difference between the two beds. However, solids circulation cannot be maintained at U_f below $2.5 U_{mf}$ (0.32 m/s) at the given initial static bed height of 0.6 m. The effect of gas velocity in the moving bed (U_m) on W_s is shown in Fig. 4B. The solids circulation rate increases with increasing U_m since moving bed voidage increases with U_m , which provides more free flow of solids in the bed. As can be seen, solids circulation cannot be attained at U_m below $0.34 U_{mf}$ (0.04 m/s). However, W_s increases significantly with the further increase of U_m up to about $0.61 U_{mf}$ (0.08 m/s). On the other hand, a dead zone at the opposite corner from the orifice side was observed when U_m is lower than U_{mf} . However, the dead zone area decreases with increasing U_m .

The measured W_s has been correlated with the gas velocities in the fluidized and moving beds since the

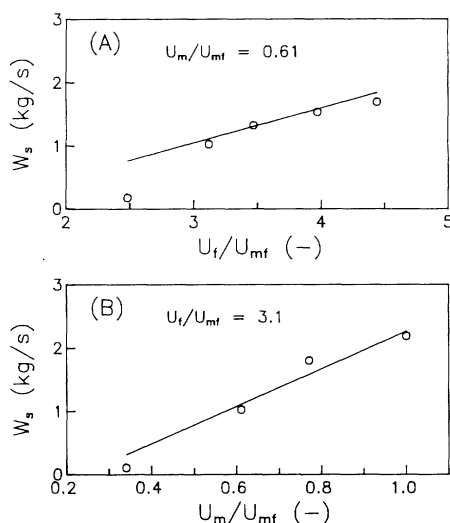


Fig. 4. (A) Effect of U_f on W_s . (B) Effect of U_m on W_s . (—): Eq. (5)

present orifice opening area was so large that the orifice equation did not represent solids flow rate well.¹¹⁾

$$W_s = 1.48(U_f/U_{mf})(U_m/U_{mf}) - 0.35(U_f/U_{mf}) - 1.65(U_m/U_{mf}) + 0.39 \quad (5)$$

with a correlation coefficient of 0.96.

2.2 Bubble properties

The bubble properties were measured at different axial and lateral positions in the fluidized bed with an initial static bed height of 0.6 m.

Bubble size distribution Bubble size distributions have been represented by the normal,¹³⁾ gamma¹⁶⁾ and logarithmic normal distributions.²¹⁾ The number density distributions of the measured individual bubble chord length are well represented by the logarithmic normal distributions, which can be expressed as:

$$f(l_{vi}) = \frac{1}{\sqrt{2\pi}l_{vi}\beta} \exp\left[-\frac{(\ln l_{vi} - \alpha)^2}{2\beta^2}\right] \quad (6)$$

where α and β are logarithmic geometric mean bubble chord length and its geometric standard deviation respectively.

The measured individual bubble chord length distributions are shown in Fig. 5. As can be seen, the distributions are widened with bed height since the bubble coalescence proceeds along the bed height.

Bubble chord length The mean bubble chord length (\bar{l}_v) was defined as the mean value of the distribution function from Eq. (6) as:

$$\bar{l}_v = \exp(\alpha + 0.5\beta^2) \quad (7)$$

where α and β are the parameters for the measured bubble chord length distribution function as evaluated by a nonlinear regression analysis.

The measured \bar{l}_v at the bed center along the bed

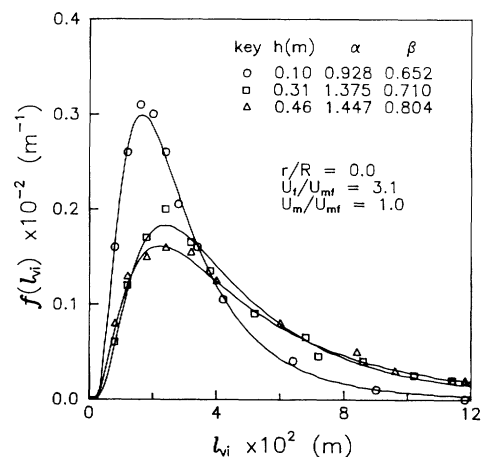


Fig. 5. Distributions of measured individual bubble chord length

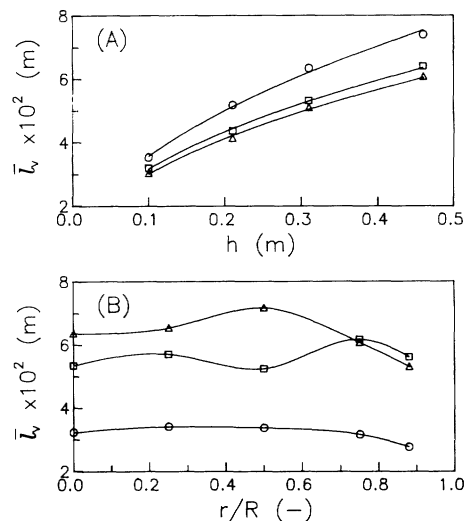


Fig. 6. (A) Variation of bubble chord length with bed height

($r/R=0.0$, $U_f/U_{mf}=3.1$)

U_m/U_{mf} : (○) 0.34; (□) 0.71; (△) 1.0

(B) Variation of bubble chord length with lateral positions

($U_f/U_{mf}=4.0$, $U_m/U_{mf}=0.61$)

h : (○) 0.1 m; (□) 0.31 m; (△) 0.46 m

height (h) is shown in Fig. 6A. As can be expected, \bar{l}_v increases with increasing h due to the bubble coalescence. However, \bar{l}_v decreases with increasing W_s at the same h and U_f due to vigorous solid mixing which may cause bubble breakup in the bed, especially below the partition plate. In a moving fluidized bed, Bolton and Davidson¹⁾ proposed that the excess gas velocity ($U - U_{mf}$), which is responsible for bubble growth in fluidized bed based on the two-phase theory of fluidization, should be replaced by the corrected excess gas velocity ($U' - U_{mf}$) in fluidized beds with solids circulation as:

$$U' - U_{mf} = U - V_s \varepsilon_{mf} / (1 - \varepsilon_{mf}) - U_{mf} \quad (8)$$

where V_s is the superficial solids velocity ($W_s/\rho_s A_f$)

and $V_s \varepsilon_{mf} / (1 - \varepsilon_{mf})$ represents the gas flow entrained by the emulsion phase. Thus, the effect of excess gas velocity on bubble growth is reduced due to the solids circulation, which may cause bubble size reduction with increasing W_s .

The variation of \bar{l}_v with lateral position in the bed is shown in Fig. 6B. The bubble chord length is found to be independent of lateral position at a bed height of 0.1 m. However, it exhibits a peak value at $r/R = 0.5-0.8$ and the peak moves to the center of the bed at higher bed heights. This may indicate that the solid particles are carried up by the bubbles in the annular region and descend mainly near the bed wall region.²²⁾

Bubble rising velocity Davidson and Harrison⁶⁾ proposed the absolute bubble rising velocity (U_b) as:

$$U_b = U - U_{mf} + U_{br} \quad (9)$$

where U_{br} is a single bubble rising velocity that can be expressed as $0.711\sqrt{gD_e}$ in the bubbly flow regime,⁶⁾ and $0.35\sqrt{gD}$ in the slug flow regime.⁷⁾

For the fluidized bed with solids circulation, Bolton and Davidson¹⁾ proposed U_b as the following relation.

$$U_b = [U - U_{mf} + V_s] + U_{br} \quad (10)$$

in which U_b in the present study was determined from the relationship between l_{vi} and U_{bi} as shown in Eqs. (2) and (3).

The variation of U_b at the bed center along the bed height (h) is shown in Fig. 7. As can be seen, U_b increases with increasing h and U_f at lower bed heights since U_b increases with h due to bubble coalescence along the bed height, and U_b increases with U_f due to the increase of V_s . However, the rate of increase of U_b decreases with increasing h due to slug formation which was observed above about 0.3 m from the distributor as reported by Werther and Molerus,²²⁾ who noted that bubble size was larger but its rising velocity was slower due to increasing wall effect in the slugging bed.

Relationship between bubble size and velocity To compare the bubble sizes in terms of equivalent bubble diameter (D_e), it is necessary to convert the mean bubble chord length (\bar{l}_v) to D_e . The relationship between \bar{l}_v and D_e depends on the bubble shape. Hemispherical-cap bubbles were observed in the present study.

The following relationship between \bar{l}_v and D_e can be made on the basis of the bubble shape proposed by Rowe and Masson¹⁵⁾ as:

$$D_e = 1.63\bar{l}_v \quad (11)$$

Also, Hovmand and Davidson⁷⁾ reported that U_b is governed mainly by the bed diameter (D) rather than by the bubble size when D_e/D is larger than about 1/3. As can be seen in Fig. 8, the rate of increase in

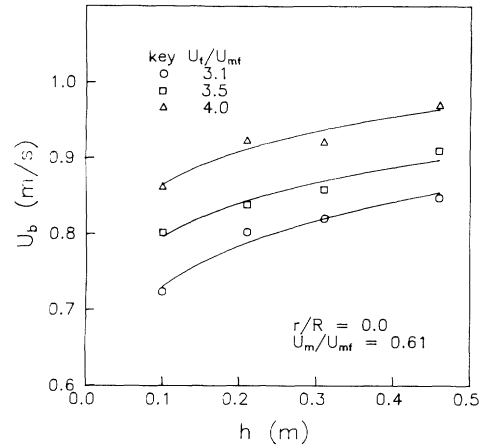


Fig. 7. Variation of bubble rising velocity with bed height

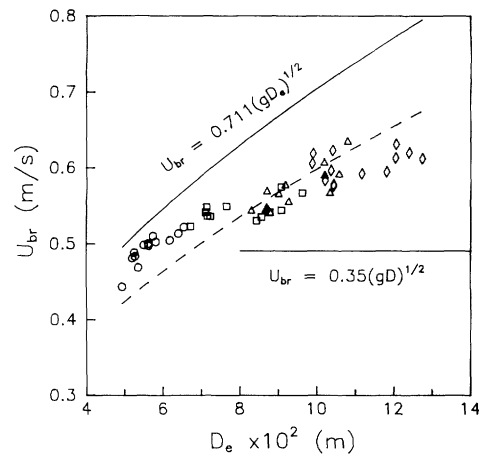


Fig. 8. Relationship between a single bubble rising velocity and equivalent bubble diameter

h : (○) 0.1 m; (□) 0.2 m; (△) 0.31 m; (◇) 0.46 m

U_{br} increases with D_e less than 0.07 m, and then the rate decreases with further increase in D_e since the flow regime lies between the bubbly and slug flow regimes (Eq. 12).

The relationship between U_{br} and D_e can be represented as:

$$U_{br} = 0.605\sqrt{gD_e} \quad (12)$$

with a correlation coefficient of 0.93.

Bubble volume fraction The variation of ε_b at the bed center with gas velocity (U_m) at various bed heights (h) is shown in Fig. 9A. As can be expected, ε_b increases with bed height above the distributor due to bubble coalescence. However, ε_b decreases with increasing U_m at the same h and U_f since bubble size decreases with increasing W_s . The variation of ε_b with lateral position in the bed is shown in Fig. 9B. As can be seen, ε_b is lower in the bed wall region and exhibits a peak value at $r/R = 0.5-0.8$, and the peak moves to the center of the bed at higher bed heights²³⁾ as in the case of bubble size.

For a fluidized bed with solids circulation,

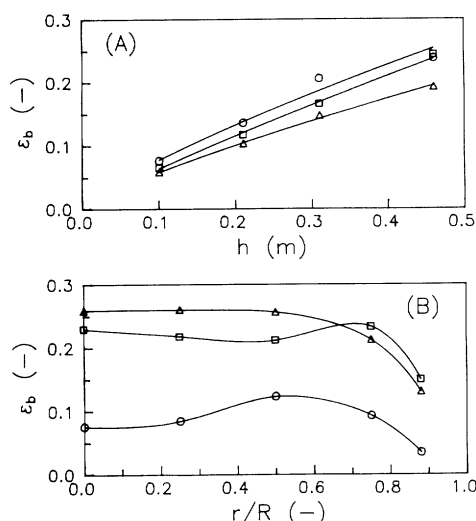


Fig. 9. (A) Variation of bubble volume fraction with bed height ($r/R=0.0$, $U_f/U_{mf}=3.1$)
 U_m/U_{mf} : (○) 0.34; (□) 0.71; (△) 1.0
 (B) Variation of bubble volume fraction with lateral position ($U_f/U_{mf}=4.0$, $U_m/U_{mf}=0.61$)
 h : (○) 0.1 m; (□) 0.31 m; (△) 0.46 m

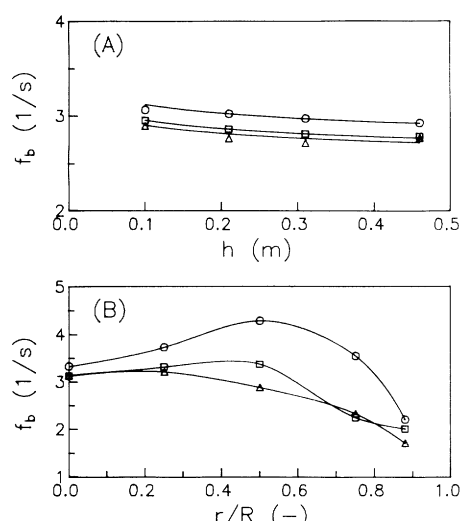


Fig. 10. (A) Variation of local bubble frequency with bed height ($r/R=0.0$, $U_f/U_{mf}=3.1$)
 U_m/U_{mf} : (○) 0.34; (□) 0.71; (△) 1.0
 (B) Variation of local bubble frequency with lateral position ($U_f/U_{mf}=4.0$, $U_m/U_{mf}=0.61$)
 h : (○) 0.1 m; (□) 0.31 m; (△) 0.46 m

LaNauze¹¹⁾ considered a slug rising velocity relative to the moving emulsion phase and proposed the following relationship of ε_b :

$$\varepsilon_b = \frac{U' - U_{mf}}{U + V_s - U_{mf} + U_{br}} \quad (13)$$

Based on Eq. (13), the present experimental data of ε_b with Eq. (12) yields

$$\varepsilon_b = \frac{k(U' - U_{mf})}{U + V_s - U_{mf} + U_{br}} \quad (14)$$

in which k increases with increasing bubble size since the rate of increase of U_{br} decreases with increasing bubble size and the resulting mean k value is found to be 0.503.

Local bubble frequency The effect of solids circulating rate in terms of gas velocity (U_m) in the moving bed on local bubble frequency (f_b) at the bed center along the bed height is shown in **Fig. 10A**. As can be seen, f_b decreases slightly with bed height due to bubble coalescence, and bubble frequency is found to be independent of U_m as reported by Kuramoto *et al.*¹⁰⁾ However, Yang and Keairns¹⁸⁾ reported that the solids circulation rate decreases with increase in bubble frequency in a circulating fluidized bed with draft tube.

The variation of local bubble frequency (f_b) along lateral positions in the bed is shown in **Fig. 10B**. The lateral profiles of f_b are similar to those of ε_b (**Fig. 9B**). As can be seen, f_b is lower in the bed wall region and exhibits a peak value at $r/R=0.4-0.7$, and the peak moves to the center of the bed at higher bed heights as in the case of bubble volume fraction.

Table 3. Correlations for estimating equivalent bubble diameter

Author	Correlation
Mori and Wen ¹²⁾	$D_e = D_{em} - (D_{em} - D_{eo})\exp(-0.3h/D)$
Darton <i>et al.</i> ⁵⁾	$D_e = 0.54(U - U_{mf})^{0.4}(h + 4\sqrt{A_c})^{0.8}/g^{0.2}$
Werther ²⁰⁾	$D_e = 8.53 \times 10^{-3}[1 + 27.2(U - U_{mf})]^{1/3} \times [1 + 6.84(h + h_o - h_j)]^{1.21}$
Choi <i>et al.</i> ⁴⁾	$(U - U_{mf})(D_e - D_{eo}) + 0.474g^{0.5}(D_e^{1.5} - D_{eo}^{1.5}) = 1.132(U - U_{mf})h$

Note: SI units

Local bubble frequency has been determined by Choi *et al.*⁴⁾ as:

$$f_b = 1.5k(U - U_{mf})D_{bf}^2/D_e^3 \quad (15)$$

where D_{bf} is the frontal bubble diameter and k is 0.5, assuming $D_{bf}/D_e=1.1$. The present data were fitted to Eq. (15) with the corrected superficial gas velocity (U') and the k value is found to be 0.518.

Comparison of bubble size with proposed correlations A number of correlations to predict bubble size in fluidized beds have been proposed in the literature. Typical correlations to predict the equivalent bubble diameter (D_e) in gas-solids fluidized beds are summarized in **Table 3**.

A comparison between observed and calculated bubble diameters from the correlations is shown in **Fig. 11A–11D**. The measured \bar{l}_v was converted into D_e by using Eq. (11). A comparison between experimental

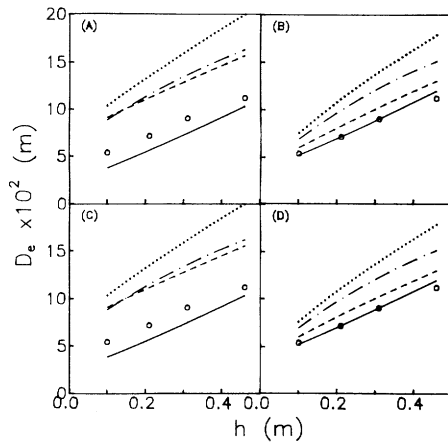


Fig. 11. (A) Comparison between measured and calculated D_e from the correlations (B) Comparison between measured and calculated D_e from the correlations using measured D_{eo} (C) Comparison between measured and calculated D_e from the correlations with modified excess gas velocity (Eq. 8) and modified bed height (Eq. 16) (D) Comparison between measured and calculated D_e from the correlations with measured D_{eo} and modified excess gas velocity (Eq. 8) and modified bed height (Eq. 16) $U_f/U_{mf}=3.1-4.5$, $U_m/U_{mf}=0.61$; (○) this study; (—) Werther²⁰⁾; (---) Mori and Wen¹²⁾; (----) Darton *et al.*,⁵⁾ (.....) Choi *et al.*,⁴⁾

and predicted D_e is shown in Fig. 11A. As can be seen, the predicted values of D_e are larger than those of the experimental values and the deviations between D_e increase with increasing bed height. This deviation may be attributed to the initial bubble diameter (D_{eo}) at the distributor. In the present study, D_{eo} at the bubble cap distributor is found to be smaller than that of the correlations except the one of Werther,²⁰⁾ who used a bubble cap distributor that distributes gas radially from each inlet port, producing smaller bubbles than would a single orifice.⁵⁾ A comparison between the present values and the values of D_e predicted from the correlations considering D_{eo} is shown in Fig. 11B. As can be seen, the predicted values are larger than the experimental values of the present study due to the solids circulation. Bolton and Davidson¹⁾ reported that bubble growth depends on how much fluidized material a bubble passed through rather than the absolute distance which a bubble travelled. Therefore, they¹⁾ proposed that a modified bed height (h') should be considered in each correlation to take account of solids circulation:

$$h' = \frac{U' - U_{mf} + U_{br}}{U + V_s - U_{mf} + U_{br}} h \quad (16)$$

The value of D_e in each correlation can be calculated with the corrected superficial gas velocity (Eq. 8) and the modified bed height (Eq. 16) by an iterative procedure.

A comparison between the measured and predicted values of D_e from the correlations considering the movement of emulsion phase is shown in Fig. 11C. As can be seen, the deviations between the measured and predicted values from the correlations become larger than those where D_{eo} is considered (Fig. 11B). Thus, D_{eo} is an important parameter in predicting the bubble size in gas-fluidized beds. The values of D_e predicted from the correlations considering both D_{eo} and the movement of emulsion phase are shown in Fig. 11D. As can be seen, the deviations become smaller and the values predicted from the correlation of Werther²⁰⁾ are well in accord with the present experimental data at lower bed heights. However, agreement becomes poorer at higher bed heights.

Correlation of bubble size The flow regime of the present study lies in the transition between the bubbling and slugging regimes, and the rate of increase of bubble size with bed height is smaller than that reported by Choi *et al.*⁴⁾ due to the solids circulation in the bed. Therefore, bubble size in the present circulating fluidized bed can be correlated with the solids circulation rate based on the theoretical correlation of Choi *et al.*,⁴⁾ which was based on the collision theory with random spatial bubble distribution as:

$$(U' - U_{mf})(D_e - D_{eo}) + 0.403g^{1/2}(D_e^{1.5} - D_{eo}^{1.5}) = 0.503(U' - U_{mf})h' \quad (17)$$

in which D_{eo} has been correlated with the excess gas velocity and catchment area (A_c) as proposed by Darton *et al.*⁵⁾ as:

$$D_{eo} = 0.13[(U' - U_{mf})A_c/g^{1/2}]^{0.22} \quad (18)$$

with a correlation coefficient of 0.93.

The bubble size can be estimated from Eqs. (5), (8) and (16), and Eq. (17) covers the range of variables $3.1 < U_f/U_{mf} < 4.5$, $0.6 < U_m/U_{mf} < 1.0$, and $0 < h < 0.46$ m.

Conclusions

In an internally circulating fluidized bed, the solids circulation rate increases with increasing gas velocity to the fluidized and moving beds. The measured bubble chord length distribution has been represented by a logarithmic normal distribution. The measured bubble chord length, volume fraction and bubble rising velocity increase with bed height and gas velocity to the fluidized bed. However, bubble chord length, volume fraction and local bubble frequency decrease with increasing gas velocity to the moving bed. The bubble properties are lower in the bed wall region and exhibit a peak value at $r/R=0.5-0.8$ and the peak moves to the center region of the bed with increasing bed height. The bubble rising velocity decreases with

equivalent bubble diameter above about 0.07 m, at which the flow regime may lie between bubbly and slugging flows.

Acknowledgement

We acknowledge a grant-in-aid for research from the Ministry of Science and Technology of Korea.

Nomenclature

A_c	= catchment area for a bubble at the distributor	[m ²]
A_f	= cross-sectional area of a fluidized bed	[m ²]
A_m	= cross-sectional area of a moving bed	[m ²]
D	= hydraulic bed diameter	[m]
D_{bf}	= frontal bubble diameter	[m]
D_e	= equivalent bubble diameter	[m]
D_{em}	= maximum bubble diameter	[m]
D_{eo}	= initial bubble diameter	[m]
f_b	= local bubble frequency	[1/s]
$f(l_{vi})$	= number density distribution of individual bubble chord length	[1/m]
g	= gravitational acceleration	[m/s ²]
h	= bed height above distributor	[m]
h'	= corrected bed height above distributor	[m]
h_j	= height of bubble formation	[m]
h_o	= equivalent height above a porous plate for $D_e = D_{eo}$	[m]
L	= distance between two thermistor probes	[m]
\bar{L}_v	= mean bubble chord length	[m]
l_{vi}	= individual bubble chord length	[m]
N_b	= number of bubbles	[—]
r	= distance from bed center-line	[m]
R	= distance between bed center-line and bed wall	[m]
ΔS	= distance between two tips of optical-fiber probe	[mm]
t	= time	[s]
T	= total measuring time	[s]
t_1	= time lag between two tips of optical probe	[s]
t_2	= duration time of a bubble pulse	[s]
U	= total superficial gas velocity in the fluidized bed	[m/s]
U'	= corrected total superficial gas velocity in the fluidized bed	[m/s]
U_b	= bubble rising velocity relative to the bed wall	[m/s]
U_{bi}	= individual bubble rising velocity	[m/s]
U_{br}	= single bubble rising velocity	[m/s]
U_f	= superficial velocity of gas supplied to the fluidized bed	[m/s]
U_m	= superficial velocity of gas supplied to the moving bed	[m/s]
U_{mf}	= minimum fluidizing gas velocity	[m/s]
V_m	= particle downward velocity in the moving bed	[m/s]
V_s	= solids superficial velocity in the fluidized bed	[m/s]
W_s	= solids circulation rate between two beds	[kg/s]

ε_b	= bubble volume fraction	[—]
ε_m	= bed voidage in the moving bed	[—]
ε_{mf}	= bed voidage at minimum fluidizing condition	[—]
ρ_s	= solid density	[kg/m ³]
τ	= time lag of signals detected by thermistor probes	[s]

<Subscript>

b	= bubble
f	= fluidized bed
i	= individual
m	= moving bed
s	= solid

Literature Cited

- 1) Bolton, L. W. and J. F. Davidson: *Chem. Eng. Commun.*, **62**, 31 (1987).
- 2) Calderbank, P. H., J. Pereira and J. M. Burgess: *Fluidization Technology*, D. L. Keairns (ed.), Hemisphere Publ. Corp., Washington D.C. Vol. I, p. 115 (1976).
- 3) Chan, I. H., C. Sishla and T. M. Knowlton: *Powder Technol.*, **53**, 217 (1987).
- 4) Choi, J. H., J. E. Son and S. D. Kim: *J. Chem. Eng. Japan*, **21**, 171 (1988).
- 5) Darton, R. C., R. D. LaNauze, J. F. Davidson and D. Harrison: *Trans. Inst. Chem. Engrs.*, **55**, 274 (1977).
- 6) Davidson, J. F. and D. Harrison: *Fluidized Particles*, Cambridge University Press, New York (1963).
- 7) Hovmand, S. and J. F. Davidson: *Fluidization*, J. F. Davidson and D. Harrison (eds.), Academic Press, London, p. 193 (1971).
- 8) Kunii, D. and O. Levenspiel: *Fluidization Engineering*, John Wiley & Sons, Inc., New York (1969).
- 9) Kunii, D.: *Chem. Eng. Sci.*, **35**, 1887 (1980).
- 10) Kuramoto, M., D. Kunii and T. Furusawa: *Powder Technol.*, **47**, 141 (1986).
- 11) LaNauze, R. D.: *Powder Technol.*, **15**, 117 (1976).
- 12) Mori, S. and C. Y. Wen: *AIChE J.*, **21**, 109 (1975).
- 13) Park, W. H., W. K. Kang, C. E. Capes and G. L. Osberg: *Chem. Eng. Sci.*, **24**, 851 (1969).
- 14) Rowe, P. N. and D. F. Everett: *Trans. Inst. Chem. Engrs.*, **50**, 42 (1972).
- 15) Rowe, P. N. and H. Masson: *Trans. Inst. Chem. Engrs.*, **59**, 177 (1981).
- 16) Rowe, P. N. and C. Yacono: *Trans. Inst. Chem. Engrs.*, **53**, 59 (1975).
- 17) Tsutsui, T. and T. Miyauchi: *Int. Chem. Eng.*, **20**, 386 (1980).
- 18) Yang, W. C. and D. L. Keairns: *AIChE Symp. Ser.*, **74**, 218 (1978).
- 19) Valenzuela, J. A. and L. R. Glicksman: *Powder Technol.*, **38**, 63 (1984).
- 20) Werther, J.: *Fluidization*, J. F. Davidson and D. L. Keairns (eds.), Cambridge Univ. Press, London, 7 (1978).
- 21) Werther, J.: *Trans. Inst. Chem. Engrs.*, **52**, 149 (1974).
- 22) Werther, J. and O. Molerus: *Int. J. Multiphase Flow.*, **1**, 123 (1973).
- 23) Wittmann, K., H. Helmrich and K. Schügerl: *Chem. Eng. Sci.*, **36**, 1673 (1981).